Nanomaterials

Site-Specific Photodeposition of Silver on ZnO Nanorods**

*Claudia Pacholski, Andreas Kornowski, and Horst Weller**

In recent years the optical and electronic properties of semiconductor and metal nanoparticles were intensively investigated and their functionality was improved by forming hybrid materials.[1–3] Great progress was made in coating nanoparticles with an appropriate material to increase the stability and to control the properties.[3–7] These nanocomposites have proven to be useful for a lot of applications such as biolabels, electroluminescent displays, memory devices, photochemical solar cells, and sensors.[8–12]

The combination of semiconductor and metal nanoparticles is particularly interesting for catalytic applications. Both the photochemical removal of contaminants from waste stream water and the optimization of the water-splitting reaction require high photocatalytic activity of the nanoparticles.[13] In general the photocatalytic efficiency is limited by the fast recombination of the photogenerated charge carriers. In semiconductor/metal nanocomposites the photoinduced charge carriers are trapped by the noble metal, which promotes interfacial charge-transfer processes.[14,15] Thus, the photocatalytic performance was improved by deposition of metal or metal islands on TiO_2 or ZnO nanoparticles.[16]

In addition to the preparation of core/shell particles, the construction of complex nanostructures by self-organization also expands the scope of composite nanoclusters to a wide range of applications.[17] Strategies for the formation of superlattices and macroscopic solids consisting of two- or three-dimensional periodic structures include the utilization of electrostatic interactions between positively and negatively charged nanoparticles, covalent linkage of particles, magnetic forces, as well as interparticle van der Waals forces. In the latter case colloidal crystals from CdSe, FePt, and $CoPt_3$ with sizes of up to 200 μm could be prepared by using the method of controlled oversaturation. The growth of the crystals was induced by slow diffusion of a non-solvent into a concentrated solution of nanocrystals.[18,19] A very promising approach is the biomolecule-driven assembly of nanoparticles that were functionalized with, for example, single-stranded DNA or biotin prior to the self-assembly process.[20] In the most advanced form this concept requires anisotropic nanoparticles, which can be functionalized with different molecular recognition groups at specific positions on the nanoparticles. Such anisotropic microrods encoded with sub-μm stripes of metals and molecules were synthesized by sequential electrochemical depositions inside porous templates and have been immobilized on Au films through selective DNA hybridization.[21,22]

In contrast, the utilization of the intrinsic properties of nanocrystals for their assembly has so far not been investigated in detail even though the dependence of both the adsorption of molecules on bulk surfaces and the different reactivity of the crystallographic facets is well known in surface science.[23,24] First attempts to transfer this knowledge from surface science to nanoparticles led to promising results. For example, the synthesis of CdSe nanorods is based on the different adsorption behavior of ligands on the crystallographic facets and the resulting differences in the growth rates.[25,26] El-Sayed et al. have demonstrated laser-induced shape changes of colloidal gold nanorods. This behavior of the gold particles was explained by the different stability of the crystallographic facets.[27,28] Comparable results were achieved by Murphy et al. who investigated the effect of nanoparticle shape on their chemical behaviour. The results indicated that gold spheroids are more stable than spheres and nanorods with regard to their dissolution.[29]

We report here a novel method for the formation of a nanoheterostructure consisting of a ZnO nanorod with an attached spherical Ag particle at one end. This material is easily accessible by the anisotropic photoreduction of Ag^+ ions at the ZnO.

The electronic structure of semiconductors such as zinc oxide is characterized by a valence band, which is filled with electrons, and an empty conduction band. Upon light absorption an electron is promoted from the valence band into the conduction band. The generated hole in the valence band and the conduction band electron can react with electron donors and electron acceptors adsorbed on the semiconductor surface, respectively.[30,31] Thus, irradiation of a

[*] Dr. C. Pacholski, Dipl.-Ing. A. Kornowski, Prof. Dr. H. Weller
University of Hamburg
Institute of Physical Chemistry
Grindelalle 117, 20146 Hamburg (Germany)
Fax: (+49) 40-42838-3452
E-mail: weller@chemie.uni-hamburg.de

[**] This work was partially funded by the European Commission through the IST-FET Nanotechnology Information Devices initiative, BIOAND project IST-1999-11974.

Supporting information for this article is available on the WWW under http://www.angewandte.org or from the author.

  DOI: 10.1002/ange.200453880

solution of ZnO nanoparticles in ethanediol/water containing metal ions leads to metal nanoparticle formation by reduction by the conduction band electrons, and concomitantly to an oxidation of the alcohol by valence band holes.

Figure 1a shows a TEM image of the solution after irradiation. The silver particles can clearly be distinguished from the ZnO nanorods by shape and contrast. In all cases the

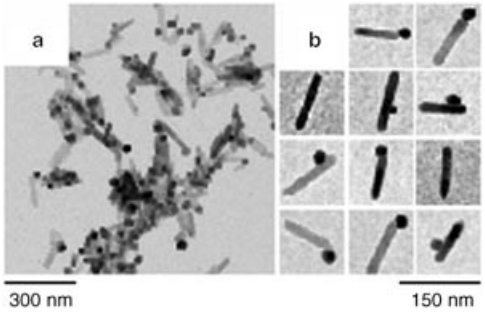

Figure 1. TEM images of Ag^+-containing ZnO nanorod solutions after irradiation. a) ZnO nanorods with deposited silver particles. b) Irradiation experiment with poly(ethylenimine) as stabilizer.

silver particles are quite polydisperse; prolonged irradiation increases the polydispersity. A detailed inspection of the image shows that not more than one Ag particle per ZnO rod is formed, and the Ag particles are preferentially located at one end of the ZnO nanorods. The latter finding is more clearly seen in the case of longer ZnO rods. To achieve a better separation of the ZnO/Ag nanocomposites on the TEM grid a stabilizer (poly(ethylenimine)) was added to the reaction solution before irradiation.[32] The corresponding TEM images are depicted as a gallery of typical selected area images in Figure 1b and also in the Supporting Information. These images strongly suggest that the photoreduction preferentially occurs at one end of the ZnO nanorods and that once a Ag nucleus is formed further reduction of Ag at this nucleus is clearly favored over nucleation.

These results can be explained in different ways. The most trivial explanation is based on drying effects during the preparation of the TEM grids. In this case silver particles would be formed homogeneously in solution and a specific interaction between the crystalline facets and the bottom or the top of the nanorod would lead to the observed nanoheterostructures. However, Figure 1b strongly contradicts this hypothesis since the images were taken at low coverage. Further evidence against this mechanism was also found in absorption and fluorescence investigations during Ag formation. Figure 2 shows the absorption spectra of ZnO nanorods (20 nm × 6 nm) at different times after reduction of silver ions. One clearly recognizes that the typical ZnO absorption becomes more and more superimposed by the growing silver plasmon band with a maximum around 440 nm. The corresponding fluorescence spectra are displayed in the inset of Figure 2. The luminescence is more and more quenched on increasing the amount of silver. Since the absorbance at the excitation wavelength (340 nm) does not significantly change during the silver reduction and the absorbance of silver is

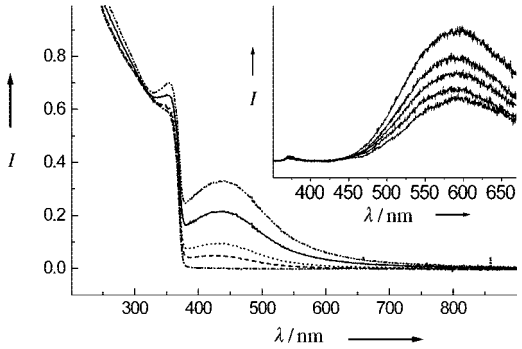

Figure 2. Evolution of the absorption spectra of an Ag^+-containing ZnO solution during irradiation. Nanorods: length 20 nm, width 6 nm. The inset shows the appropriate fluorescence spectra of the mixture.

negligible in the spectral range of the ZnO fluorescence, the quenching of the trapped emission must be due to electron transfer from ZnO to silver particles.[14]

Another explanation for the site-selective deposition of silver involves a preferentially small lattice mismatch of silver on ZnO at the respective crystallographic plane. In this case tiny Ag clusters could be formed at various sites on the ZnO nanorod, whereas nucleation of Ag particles would occur in a consecutive step at the energetically favored plane after surface diffusion. Indeed, several high-resolution TEM images show almost epitaxial growth of single-crystalline Ag particles on the ZnO nanorod substrate (Figure 3a, b). Ag particles on the ZnO moieties can clearly be distinguished by the different contrast. The lattice distances are in accord with silver and ZnO. Unfortunately, even tilt experiments in the TEM did not allow the respective crystallographic planes at

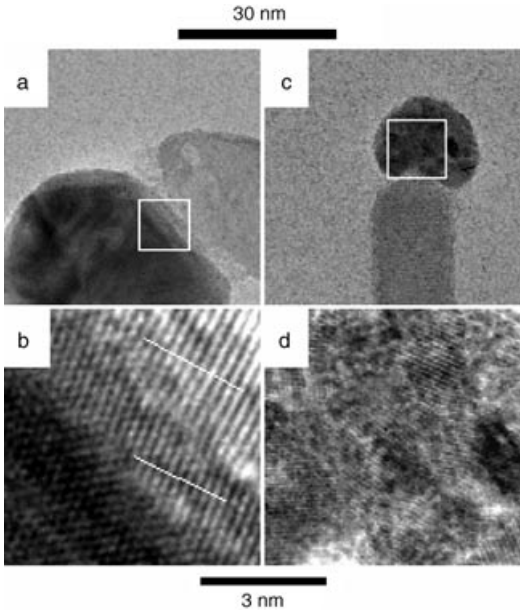

Figure 3. HRTEM images of the interface of Ag particles and ZnO nanorods. a) Epitaxially grown single-crystalline silver particle on ZnO, and b) corresponding high-resolution TEM image of the interface, c) and d) polycrystalline silver particle deposited on ZnO.

the interface of ZnO and Ag to be identified unambiguously, and therefore this mechanism remains speculative. In addition the formation of polycrystalline Ag particles at the top of the ZnO nanorods was also observed (Figure 3c, d). In this case, the epitaxial growth model is of course completely hypothetical.

Reduction of Ag at preferential crystallographic planes could also be explained by specific adsorption of Ag^+ ions at the respective plane. Literature data for aqueous solutions containing additional stabilizer molecules such as citrate and poly(ethylenimine) are, however, not available and our attempts to analyze the Ag content at the respective ZnO sites prior to the photoreduction step by energy-dispersive X-ray (EDX) and wavelength-dispersive X-ray (WDX) experiments failed due to the limited stability of the sample under intense electron illumination.

Finally one might discuss a localization of the electrons at the ends of the ZnO nanorods prior to the electron transfer step. This charge separation might be supported by an intrinsic dipole moment along the *c* axis, that is the growth direction of the rods or an asymmetric band bending along the *c* axis.[33–35] Electron density calculations of excited ZnO nanorods would be required to get further evidence for this mechanism. Which of the discussed processes is responsible for the obtained results can not be decided at this stage.

The presented results provide a rational approach for the bottom-up assembly of complex nanostructures. Indeed the here presented structure represents electronically a fully self-assembled 2D quantum-confined semiconductor with an in-built Schottky barrier. Furthermore, the chemical anisotropy might serve as branching centers for a more complex architecture of nanohybrid materials, which should have favorable charge-transport properties as compared to conventional nanoparticle solids. Also site-specific building of different ligands and molecular recognition groups such as single-stranded DNA oligonucleotides or peptides should become possible with the presented Ag/ZnO nanocomposite particles. The further development of this concept could lead to the custom-made construction of electronic and optical devices.

Experimental Section

ZnO nanorods were prepared according to a method described earlier. Briefly, zinc acetate dihydrate (29.5 g, 0.13 mol) was dissolved in methanol (125 mL) at 60 °C. Then, a solution of potassium hydroxide (14.8 g, 0.23 mol) in methanol (65 mL) was subsequently added under vigorous stirring. The size of the resulting nanorods was controlled by refluxing the reaction mixture for different times at 60 °C. Lengthening the reaction time led to a considerable increase in length along the *c* axis of the crystals, whereas the width of the rods is only slightly enlarged. Because of precipitation of the ZnO particles during the synthesis they could be easily isolated from the reaction mixture by centrifugation. Washing of the precipitated particles with methanol was necessary to remove the excess ions. After centrifugation (5500 U min^{-1}, 30 min) the resulting gel was redispersed in chloroform. For optical measurements the nanoparticles were diluted with a mixture of ethyleneglycol/water (2:1).

Silver deposition was carried out photocatalytically in quartz cells using a 450-W xenon lamp in combination with a monochromator and a band-edge filter (320 nm). A mixture of ethanediol/water (2:1, v:v; 2670 μL), ZnO nanorods (300 μL) in ethanediol/water (c = 0.01 mol L^{-1}) and $AgNO_3$ (30 μL) in water (c = 0,1 mol L^{-1} or 0.01 mol L^{-1}) was illuminated with monochromatic light (λ = 340 nm) under stirring. To separate the silver/ZnO nanocomposites on the TEM grid, a diluted poly(ethylenimine) solution (30 μL) in water was added. All experiments were carried out in degassed solutions to avoid oxygen reduction by the conduction band electrons, although significantly different results were not observed in the presence of oxygen.

Received: January 29, 2004 [Z53880]

Keywords: photochemistry · quantum dots · semiconductors · silver · zinc oxide

[1] A. Eychmüller, *J. Phys. Chem. B* **2000**, *104*, 6514 – 6528.
[2] S. Link, M. A. El-Sayed, *J. Phys. Chem. B* **1999**, *103*, 8410 – 8426.
[3] P. Mulvaney, *Langmuir* **1996**, *12*, 788 – 800.
[4] A. Dawson, P. V. Kamat, *J. Phys. Chem. B* **2001**, *105*, 960 – 966.
[5] I. Pastoriza-Santos, D. S. Koktysh, A. A. Mamedov, M. Giersig, N. A. Kotov, L. M. Liz-Marzán, *Langmuir* **2000**, *16*, 2731 – 2735.
[6] A. Wood, M. Giersig, P. Mulvaney, *J. Phys. Chem. B* **2001**, *105*, 8810 – 8815.
[7] S. Haubold, M. Haase, A. Kornowski, H. Weller, *ChemPhysChem* **2001**, *2*, 331.
[8] Jr. M. Bruchez, M. Moronne, P. Gin, S. Weiss, A. P. Alivisatos, *Science* **1998**, *281*, 2013 – 2016.
[9] A. Schroedter, H. Weller, R. Eritja, W. E. Ford, J. M. Wessels, *Nano Lett.* **2002**, *2*, 1363.
[10] M. C. Schlamp, X. Peng, A. P. Alivisatos, *J. Appl. Phys.* **1997**, *82*, 5837 – 5842.
[11] W. U. Huynh, J. J. Dittmer, A. P. Alivisatos, *Science* **2002**, *295*, 2425 – 2427.
[12] Y. Nakato, K. Ueda, H. Yano, H. Tsubomura, *J. Phys. Chem.* **1988**, *92*, 2316.
[13] D. W. Bahnemann, D. Bockelmann, R. Goslich, M. Hilgendorff in *Photocatalytic detoxification of polluted aquifers: Novel catalysts and solar applications, Vol. 1* (Eds.: D. W. Bahnemann, D. Bockelmann, R. Goslich, M. Hilgendorff) Lewis Publishers, Boca Raton, Ann Arbor, London, Tokyo, **1994,** pp. 349 – 367.
[14] V. Subramanian, E. E. Wolf, P. V. Kamat, *J. Phys. Chem. B* **2003**, *107*, 7479 – 7485.
[15] M. Jakob, H. Levanon, P. V. Kamat, *Nano Lett.* **2003**, *3*, 353.
[16] T. Abe, E. Suzuki, K. Nagoshi, K. Miyashita, M. Kaneko, *J. Phys. Chem. B* **1999**, *103*, 1119 – 1123.
[17] A. N. Shipway, E. Katz, I. Willner, *ChemPhysChem* **2000**, *1*, 18 – 52.
[18] D. V. Talapin, E. V. Shevschenko, A. Kornowski, N. Gaponik, M. Haase, A. L. Rogach, H. Weller, *Adv. Mater.* **2001**, *13*, 1868 – 1871.
[19] E. V. Shevchenko, D. V. Talapin, A. Kornowski, F. Wiekhorst, J. Kötzler, M. Haase, A. L. Rogach, H. Weller, *Adv. Mater.* **2002**, *14*, 287 – 290.
[20] R. C. Mucic, J. J. Storhoff, C. A. Mirkin, R. L. Letsinger, *J. Am. Chem. Soc.* **1998**, *120*, 12674 – 12675.
[21] D. J. Pena, B. Razavi, P. A. Smith, J. K. Mbindyo, M. J. Natan, T. S. Mayer, T. E. Mallouk, C. D. Keating, *Mater. Res. Soc. Symp. Proc.* **2001**, *636*, D4.6.1-D4.6.6.
[22] B. D. Reiss, J. N. K. Mbindyo, B. R. Martin, S. R. Nicewarner, T. E. Mallouk, M. J. Natan, C. D. Keating, *Mater. Res. Soc. Symp. Proc.* **2001**, *635*.
[23] P. A. M. Hotsenpiller, J. D. Bolt, W. E. Farneth, J. B. Lowekamp, G. S. Rohrer, *J. Phys. Chem. B* **1998**, *102*, 3216 – 3226.
[24] O. Dulub, L. A. Boatner, U. Diebold, *Surf. Sci.* **2002**, *519*, 201 – 217.

[25] X. Peng, L. Manna, W. Yang, J. Wickham, E. Scher, A. Kadavanich, A. P. Alivisatos, *Nature* **2000**, *404*, 59 – 61.
[26] L. Manna, E. C. Scher, A. P. Alivisatos, *J. Am. Chem. Soc.* **2000**, *122*, 12700 – 12706.
[27] S. Link, C. Burda, B. Nikoobakht, M. A. El-Sayed, *J. Phys. Chem. B* **2000**, *104*, 6152 – 6163.
[28] Z. L. Wang, R. P. Gao, B. Nikoobakht, M. A. El-Sayed, *J. Phys. Chem. B* **2000**, *104*, 5417 – 5420.
[29] N. R. Jana, L. Gearheart, S. O. Obare, C. J. Murphy, *Langmuir* **2002**, *18*, 922 – 927.
[30] D. W. Bahnemann, *Isr. J. of Chem.* **1993**, *33*, 115 – 136.
[31] S. Chen, U. Nickel, *J. Chem. Soc. Faraday Trans.* **1996**, *92*, 1555 – 1562.
[32] A. Henglein, *Chem. Mater.* **1998**, *10*, 444 – 450.
[33] S. A. Empedocles, M. G. Bawendi, *Science* **1997**, *278*, 2114 – 2117.
[34] V. L. Colvin, A. P. Alivisatos, *J. Chem. Phys.* **1992**, *97*, 730 – 733.
[35] M. Shim, P. Guyot-Sionnest, *J. Chem. Phys.* **1999**, *111*, 6955 – 6964.

